Direct Vibrational Energy Transfer in Monomeric Water Probed with Ultrafast Two Dimensional Infrared Spectroscopy

De-xia Zhou, Qian-shun Wei, Hong-tao Bian, and Jun-rong Zheng

View Online   Export Citation

ARTICLE

Direct Vibrational Energy Transfer in Monomeric Water Probed with Ultrafast Two Dimensional Infrared Spectroscopy[†]

De-xia Zhou[a], Qian-shun Wei[a], Hong-tao Bian[a*], Jun-rong Zheng[b*]

a. Key Laboratory of Applied Surface and Colloid Chemistry of Ministry of Education, School of Chemistry and Chemical Engineering, Shaanxi Normal University, Xi'an 710119, China
b. Beijing National Laboratory for Molecular Sciences, College of Chemistry and Molecular Engineering, Peking University, Beijing 100871, China

Vibrational relaxation dynamics of monomeric water molecule dissolved in d-chloroform solution were revisited using the two dimensional Infrared (2D IR) spectroscopy. The vibrational lifetime of OH bending in monomeric water shows a bi-exponential decay. The fast component (T_1=(1.2±0.1) ps) is caused by the rapid population equilibration between the vibrational modes of the monomeric water molecule. The slow component (T_2=(26.4±0.2) ps) is mainly caused by the vibrational population decay of OH bending mode. The reorientation of the OH bending in monomeric water is determined with a time constant of τ=(1.2±0.1) ps which is much faster than the rotational dynamics of water molecules in the bulk solution. Furthermore, we are able to reveal the direct vibrational energy transfer from OH stretching to OH bending in monomeric water dissolved in d-chloroform for the first time. The vibrational coupling and relative orientation of transition dipole moment between OH bending and stretching that effect their intra-molecular vibrational energy transfer rates are discussed in detail.

Key words: Vibrational energy transfer, Confined water, Ultrafast Infrared spectroscopy, Monomeric water

I. INTRODUCTION

Water science has been the frontier of physics, chemistry, environmental science and biology studies. The hydrogen bond network of water molecule is crucial for its peculiar physical and chemical properties [1–3]. However, in most of the biological related living systems, the hydrogen bond of water molecule is encountered by the biomolecules and disrupted in the confined environments [4–15]. The structure and dynamics of water molecule in the nanometer-scale confinement showed distinct behavior compared with water in its bulk solution [16, 17]. Understanding the vibrational energy relaxation mechanism of water molecules in confined environment is essential to unravel many important biological functions that involve the surrounding hydration shell of water molecules [18].

The ultrafast relaxation dynamics of neat liquid water have been extensively studied using ultrafast IR spectroscopy in the past decades [1, 17, 19–21]. It is generally true that the vibrational relaxation dynamics is fast (less than 2 ps) due to the complex hydrogen bonds in bulk water solution [22, 23]. The short population lifetimes in neat water make the vibrational energy relaxation and dissipation pathway experimentally difficult to access. While the relaxation time constants usually can range from 2 ps to 100 ps for the water molecules in the confined environments, such as water molecules dissolved in the organic solvents [24–30]. The monomeric water thus provides a model system to study the detailed vibrational relaxation pathway. Seifert and coworkers investigated the vibrational relaxation of monomeric water in different solvents using the infrared pump probe method [24–26]. The vibrational relaxation pathway of the OH stretching in monomeric water was proposed where the overtone mode of OH bending is involved as an intermediate step [25]. However, as the author pointed out, the two dimensional Infrared (2D IR) spectroscopy with access to all vibrational modes is needed for the comprehensive analysis of vibrational energy relaxation in monomeric water.

In our previous studies, we developed the mode-specific vibrational energy transfer method based on the 2D IR spectroscopy and successfully applied this method to the electrolyte aqueous solution systems [31–36]. Following the experimental and data analysis procedures established in our previous reports, we investigated the vibrational relaxation dynamics of monomeric

water molecule dissolved in d-chloroform solution using the 2D IR spectroscopy. The vibrational lifetime of OH bending in monomeric water and the vibrational relaxation mechanism from OH stretching to OH bending are revisited. Direct vibrational energy transfer from OH stretching to OH bending in monomeric water can be clearly observed. The system is a good example to demonstrate how the governing factors (*e.g.* coupling strength and energy mismatch) affect the intramolecular vibrational energy transfer in liquids.

II. EXPERIMENTS

The experimental setup for the 2D IR spectroscopy has been described elsewhere [37, 38]. Briefly, a ps amplifier and a fs amplifier are independently operated and synchronized with the same seed pulse from a Ti-sapphire oscillator. The ps amplifier pumps an OPA to produce $\sim$1 ps Mid-IR pulses with a bandwidth $\sim$18 cm^{-1} at 1 kHz repetition rate. The fs amplifier pumps another OPA to produce $\sim$140 fs Mid-IR pulses with a bandwidth $\sim$200 cm^{-1} at 1 kHz repetition rate. In the experiments, the ps IR pulse is the pump beam. The fs IR pulse is the probe beam which is frequency resolved by a spectrograph yielding the probe axis of a two dimensional (2D) IR spectrum. Scanning the pump frequency yields the other axis of the spectrum. Two polarizers are added into the probe beam path to selectively measure the parallel or perpendicular polarized signal relative to the pump beam. Vibrational lifetimes are obtained from the rotation free signal

$$P_{\text{life}} = P_{//} + 2P_{\perp} \qquad (1)$$

where $P_{//}$ and $P_{\perp}$ are parallel and perpendicular signal respectively. Rotational relaxation times are obtained from the waiting time dependent anisotropy

$$R = \frac{P_{//} - P_{\perp}}{P_{//} + 2P_{\perp}} \qquad (2)$$

All the samples were sandwiched in a home-made cell composed of two CaF$_2$ windows separated by a Teflon spacer. The thickness of the spacer was controlled at 800 μm and can be adjusted depending upon the optical densities. All the measurements were carried out at room temperature (22 °C).

All chemicals were purchased from Sigma-Aldrich Company. The residual water contained in the d-chloroform sample was removed using the molecular sieve and further verified using FTIR spectroscopy. The structure of isolated water molecule was optimized and determined with density functional theory (DFT) calculations. The DFT calculations were carried out in the Gaussian 09 program suite. The level and basis set used were Becke's three-parameter hybrid functional combined with the Lee-Yang-Parr correction functional, abbreviated as B3LYP and 6-311++G(d,p). All results reported here do not include the surrounding solvent and therefore are for the isolated molecules.
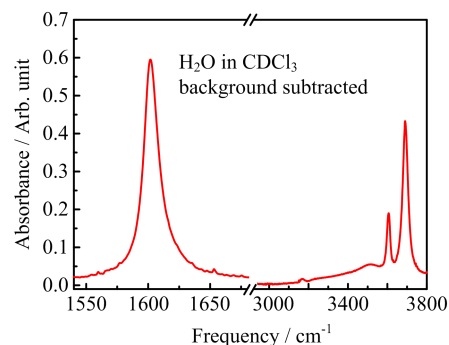
FIG. 1 FTIR spectrum of 0.04 mol/L H$_2$O dissolved in deuterated chloroform. The d-chloroform background has been subtracted.

III. RESULTS AND DISCUSSION

A. FTIR spectrum of monomeric water dissolved in organic solvent d-chloroform

Different from the water molecules in its bulk solution where each water molecule can form three dimensional hydrogen bond networks with nearby water molecules, the water molecule dissolved in organic solvent liquids is usually called the monomeric water or isolated water due to limited number of water molecules dissolved in the confined environment. FIG. 1 shows the FTIR spectrum of a 0.04 mol/L solution of H$_2$O in deuterated chloroform (CDCl$_3$) after subtracting the solvent background. The spectrum in the frequency range from 1700 cm^{-1} to 3000 cm^{-1} was not shown since there is no detectable absorption band and would not be used in the following analysis. It is clear that there are three distinct absorption bands in FIG. 1, the OH bending (ν_2) transition at 1602 cm^{-1}, the symmetric (ν_1) and asymmetric OH stretching (ν_3) vibrational bands at 3606 and 3691 cm^{-1}. Detailed peak positions, FWHM, and amplitudes are listed in Table I. Furthermore, there is a weak and broad absorption band positioned at around 3515 cm^{-1} and its origination is not clear yet. The overtone of the OH bending mode (around 3170 cm^{-1}) can be observed in our experiment but with very low absorptivity.

The isolated water dissolved in d-chloroform solution is surrounded by the organic solvent molecules and the hydrogen bond network is disrupted. Similar to the water molecules in the gas phase, the symmetric and asymmetric vibrational modes of isolated water molecule can be clearly resolved without the spectra overlapping, shown in FIG. 1. Thus we are able to perform the ultrafast vibrational dynamics of water molecules after the excitation of each specific vibrational mode and observe the vibrational energy transfer between these three vibrational modes. The vibrational relaxation dynamics of isolated water molecules in OH bending region are monitored using the 2D IR spectroscopy and mode-specific vibrational energy transfer method developed

TABLE I The peak position (in cm^{-1}), half width (in cm^{-1}) and amplitude of FTIR spectrum of monomeric water dissolved in deuterated chloroform.

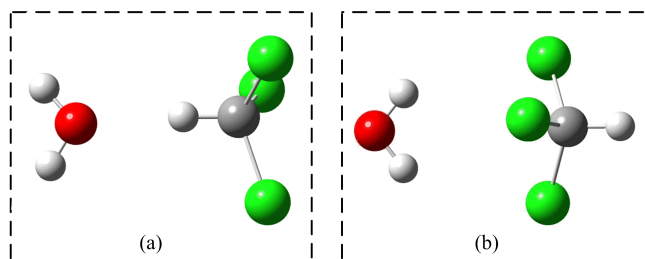| Position	Half width	Amplitude	Assignment
3691	30	0.41	Anti-symmetric
3606	19	0.16	Symmetric
1602	15	0.60	Bending

FIG. 2 Calculated complex between a water molecule and chloroform in gas phase using DFT method. Complex in (a) is more stable than that in (b) by ∼3.17 kcal/mol.

in our previous studies [34].

B. The possible structure of monomeric water dissolved in organic solvent (d-chloroform) calculated using DFT method

DFT calculation shows that the two molecules (H$_2$O and d-chloroform) can have two possible hydrogen bond configurations in the gas phase, shown in FIG. 2. The complex in FIG. 2(a) (formation energy of −4.47 kcal/mol) is more stable than the one in FIG. 2(b) (formation energy of −1.30 kcal/mol). The C−D bond in d-chloroform acting as the H-bond donor is pointing to the oxygen atom of isolated water molecule, shown in FIG. 2(a).

Here, we are more interested in the structure of water molecules affected by presence of the surrounding organic solvent molecules. In our previous reports, we have demonstrated that the three-dimensional molecular conformation of molecules in the liquid and nanoparticle systems can be determined by measuring the relative orientations of the transition dipole moments in the molecular system using the multiple mode 2D IR spectroscopy [39, 40]. It is necessary to point out that the cross angle of different vibrational modes measured from the polarization selective 2D IR is the angle between the transition dipole vectors of the two vibrational modes [37]. These vectors may or may not overlap with the chemical bonds directions. For example, the vectors of OH symmetric stretching and OH bending of water molecule are along the C$_{2v}$ symmetry axis of water molecule, while the vector of asymmetric stretch is perpendicular to the symmetric stretch. DFT calculation shows even with the presence of d-chloroform, the relative cross angles between the
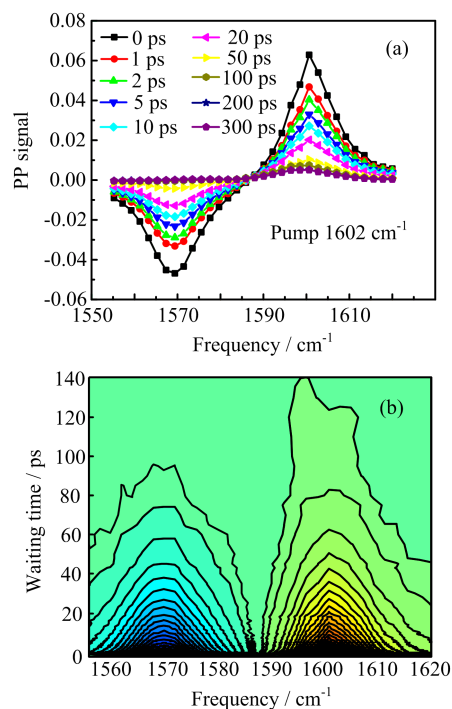

FIG. 3 (a) Transient infrared absorption spectra at parallel polarization for different pump probe delays of isolated water molecule dissolved in d-chloroform. The pump frequency is centered at 1602 cm^{-1}. (b) The contour plot of rotation free pump/probe data for isolated water in d-chloroform with the pump frequency at 1602 cm^{-1}.

three transition dipole moments of vibrational modes in monomeric water remain unchanged. *i.e.* the calculated angle between the transition dipole moments of OH bending and OH anti-symmetric stretching is 89°. Without the presence of d-chloroform, the calculated angle is 90°. Detailed analysis will be given in the following section.

C. The vibrational relaxation dynamics of monomeric water in the OH bending mode region

FIG. 3(a) shows typical transient infrared absorption spectra at different time delays of OH bending mode with the pump frequency at 1602 cm^{-1}. The 1→2 transition of OH bending (ν_2) is positioned at 1569 cm^{-1} where the anharmonicity of the OH bending mode is determined to be (33±1) cm^{-1}. FIG. 3(b) also shows the contour plot of rotation free pump/probe data for isolated water in d-chloroform. The decay of the pump probe signal (abbreviated as PP signal) is caused by the vibrational population relaxation and orientational relaxation processes. These two contributions can be separated through the polarization dependent measurement which is extensively adopted in the IR pump probe measurements. Here the heat effect from the vibrational relaxation is very small but can be observed at

longer waiting time in the $0\rightarrow1$ transition of OH bending mode. Thus the vibrational population relaxation and orientational relaxation of OH bending are analyzed using the $1\rightarrow2$ transition of the pump probe data in the OH bending region, shown in FIG. 4.

Interestingly, the vibrational lifetime of OH bending from the $v=1\rightarrow2$ transition (1569 cm^{-1}) cannot be simply described by a single exponential decay function. Thus a bi-exponential decay function is used and gives time constants of (1.2±0.1) ps (18%) and (26.4±0.2) ps (82%). The fast component T_1=(1.2±0.1) ps is possibly caused by the rapid population equilibration between the vibrational modes of the monomeric water molecule. The slow component T_2=(26.4±0.2) ps is mainly caused by the vibrational population decay of OH bending mode. Our result is different from the previous report by Seifert and coworker where a single exponential decay was used to describe the vibrational relaxation dynamics of OH bending with the time constant of (28.5±1.0) ps [24]. It is possible that the discrepancy may be caused by the different experimental setup used in different research groups. The IR pulses utilized for the IR pump probe measurement are 2.5 ps duration in the reports by Seifert *et al.* [24]. This may explain why they did not observe the bi-exponential decay of the vibrational relaxation dynamics of OH bending, since the fast component is only 1.2 ps which is much shorter than the pulse duration used in their experiment.

More importantly, we are able to determine the orientational anisotropy of OH bending of monomeric water in d-chloroform solution. A single exponential decay gives time constant of τ=(1.2±0.1) ps, shown in FIG. 4(b). However, Seifert and coworker determined the anisotropy decay of OH bending in both chloroform and d-chloroform solvents with identical time constant of τ=(2.7±0.7) ps [24]. As we mentioned in previous section, the IR pulses utilized for their IR pump probe measurement are 2.5 ps duration which are longer than the anisotropy decay and can cause the inconsistent result observed here. The rotational time constant of water in isotopically mixed bulk liquid water has been extensively studied which is observed to have a time constant of (2.6±0.1) ps [41, 42]. The much faster rotational time constant of OH bending in monomeric water observed in our report is quite surprising, because the hydrogen bonds of monomeric water in the confined environment are much weaker than the hydrogen bonds in the bulk water. Bakker *et al.* investigated the rotational dynamics of water molecules confined in the acetone molecules [43]. The rotational time constant of OH stretching in water is determined to be (6±1) ps. Interestingly, Skinner *et al.* calculated the vibrational energy relaxation rates and rotational dynamics of water in chloroform and d-chloroform using the Landau-Teller formula [28]. They did show that the rotational dynamics of water has a decay time constant of (1.2±0.1) ps. The fast rotational time constant of
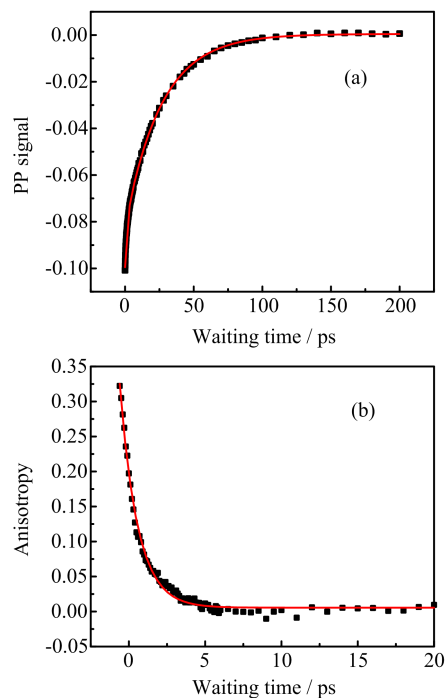

FIG. 4 (a) Vibrational and (b) rotational anisotropy decays for the $1\rightarrow2$ transition (1569 cm^{-1}) of the OH bending of isolated water in d-chloroform solution. The pump frequency is centered at 1602 cm^{-1}.

τ=(1.2±0.1) ps observed in our case may be caused by several mechanisms. The first one is that there is resonant energy transfer between the two OH groups, even the OH bending is pumped rather than the excitation of OH stretching. We will discuss the vibrational energy transfer between the OH stretching and OH bending in the following section. Secondly, the fast rotational dynamics may be related with the geometric configuration of monomeric water confined in d-chloroform. The C−D bond of d-chloroform is pointing to the oxygen atom of isolated water molecule. However, the two hydrogen atoms of isolated water molecules are not forming hydrogen bond with nearby molecules. The specific geometry of monomeric water in d-chloroform may facilitate the fast rotational dynamics. The nature of the fast rotational time constant of monomeric water molecules observed in the confined environment warrants further theoretical investigation.

D. The vibrational coupling and energy transfer between stretching and bending modes in monomeric water

FIG. 5 shows the time dependent 2D IR spectra of monomeric water molecule in d-chloroform solution with probing frequency in the OH bending region and pumping frequency in the OH stretching region. The cross peaks generated with the excitation at the OH anti-symmetric stretching is discussed. While the cross peaks excited with OH symmetric stretching is not
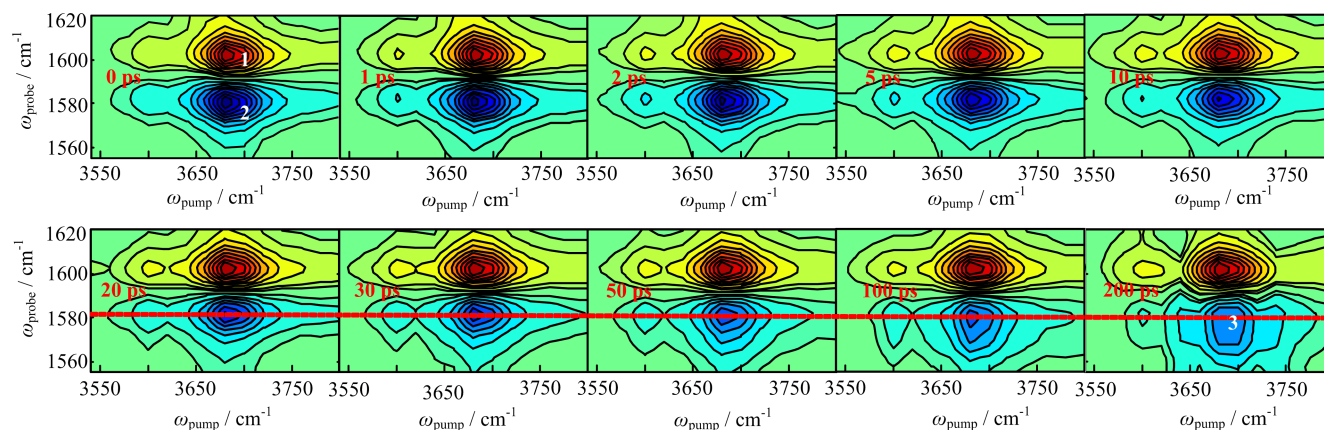
FIG. 5 Time dependent 2D IR spectra of monomeric water molecule in d-chloroform solution showing the OH bending/stretching cross peaks. Each contour is normalized to its own maximum intensity. Each contour is a 10% amplitude change. The red dashed line shows the peak position of the combination band between OH bending and OH anti-symmetric stretching.
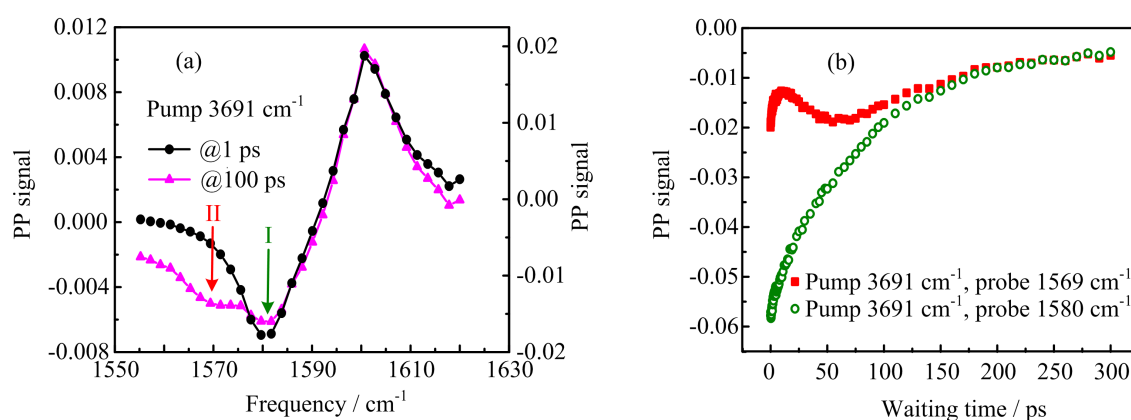

FIG. 6 (a) Transient spectra of H_2O in d-chloroform in the OH bending region with the excitation of anti-symmetric OH stretch at two different waiting times: 1 ps (square, right axis) and 100 ps (triangle, left axis). (b) Time dependent intensities of peak I (open circle) and II (solid square) in FIG. 6(a) with the excitation of anti-symmetric OH stretch at 3691 cm^{-1}.

discussed due to having the similar origination. The cross peaks generated in the positions of peaks 1 and 2 can have three possible mechanisms: coupling between OH anti-symmetric stretching/OH bending, heat effect and energy transfer from OH stretching to OH bending. The coupling between OH anti-symmetric stretching/OH bending can produce the ground state bleaching peak 1 and the combination band absorption peak 2 (1580 cm^{-1}) even at time 0. Furthermore, these two peaks should decay with the vibrational lifetime of OH stretching which is in the order to ∼80 ps [25]. The heating from the vibrational relaxation of OH stretching can also generate the cross peaks. However, the contribution of heating effect should be negligible in the monomeric water dissolved in d-chloroform solution where the water molecules are isolated without forming any aggregation. The vibrational relaxation of OH stretching energy will dissipate into the surrounding solvent molecules. The appearance of peak 3 (3691, 1569 cm^{-1}) at 100 and 200 ps in FIG. 5 demonstrates

that there is a direct vibrational energy transfer from OH stretching to OH bending.

FIG. 6(a) shows the transient spectra of H_2O in d-chloroform in the OH bending region with the excitation of anti-symmetric OH stretch at two different waiting times. At early delay time of 1 ps, the ground state bleaching peak (1602 cm^{-1}) and the combination band absorption peak (peak I, 1580 cm^{-1}) can be clearly observed, yielding an off-diagonal anharmonicity of (22±1) cm^{-1}. The results are consistent with previous reports [25]. With the increase of the waiting time at 100 ps, there is a clear indication of energy transfer peak appearing at 1569 cm^{-1} (marked with peak II). FIG. 6(b) shows the time dependent intensities of peak 2 and 3 in FIG. 5 with the excitation of anti-symmetric OH stretching at 3691 cm^{-1}. With the probe frequency at 1580 cm^{-1}, the signal shows a mono-exponential decay with a time constant of 80 ps which follows the relaxation of OH stretching mode. While with the probe frequency at 1569 cm^{-1}, the signal shows a very fast

decay up to 10 ps. Then the signal shows a steady grow and increases to a maximum at 60 ps. After that the signal decays following the relaxation of the OH stretching.

Previous study demonstrated that vibrational energy of H_2O molecules is relaxing following the scheme OH stretching→OH bending overtone→OH bending→ground state [25]. The grow of the time dependent intensity of peak II is a clear evidence showing there is a direct energy transfer from the OH stretching mode to the OH bending mode. From FIG. 5, we know there is a strong vibrational coupling between OH stretching and OH bending. However, the question raised here is that why the energy transfer rate is not efficient considering it is an intra-molecular energy transfer in monomeric water? From our previous result of the expression of mode-specific vibrational energy transfer [31], the energy transfer rate from OH stretching to OH bending is estimated to be in the range of 100 ps. The possible reasons might be related with the big energy mismatch and also the structure of monomeric water which is the relative orientation of OH stretching and OH bending. Detailed kinetic analysis of the energy transfer between OH stretching and OH bending will be given in another work. Here we only give the tentative discussion based on the measurement of the relative orientation between OH stretching and OH bending.

To determine the relative orientation of the OH stretching and OH bending of monomeric water in d-chloroform, we obtained the waiting time dependent anisotropies of the combination band (peak 2 with pump frequency of 3691 cm^{-1}), shown in FIG. 7. In two coupled modes, the anisotropy R of their combination band peak is correlated with the angle between their transition dipole moments in the form of [39]

$$R = \frac{4\cos^2\theta - 1}{5} \quad (3)$$

With initial value of R=0.18±0.02, the angle between the transition dipole moments of OH bending and OH anti-symmetric stretching is determined to be 80°±10°. According to DFT calculation, the angle between the transition dipole moments of OH bending and OH anti-symmetric stretching is calculated to be 89° which is consistent with result obtained from the anisotropy measurement. The consistency between experimental and calculated result can't be simply considered as coincidence. Even the C−D bond in d-chloroform can form hydrogen bond with water molecule shown in FIG. 2(a), it doesn't affect the structure of the monomeric water which means that the symmetry of water molecule remains unchanged. From FIG. 7, the randomization time constant of the transition dipole cross angle of the OH bending and OH anti-symmetric stretching is (0.7±0.2) ps. This constant is a little faster than the rotational time constant of the monomeric water in d-chloroform solution.
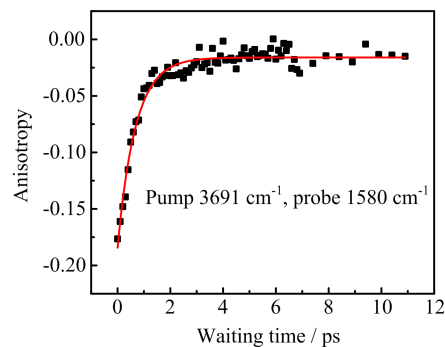
Previous study showed that vibrational relaxation

FIG. 7 Waiting time dependent anisotropies of peak 2 in FIG. 5 with pump frequency at 3691 cm^{-1} and probe frequency at 1580 cm^{-1}. The solid line is the fitting result using a single exponential decay function.

pathway of the OH stretching in monomeric water involves the overtone mode of OH bending as an intermediate step [25]. However, the direct vibrational energy transfer from OH stretching to OH bending can be observed here which shows that comprehensive analysis of vibrational energy relaxation in the monomeric water needs re-examined. We also show that the governing factors affecting the intra-molecular vibrational energy transfer are complicated than the inter-molecular vibrational energy transfer. Future studies are needed to give a clear understanding of the intra-molecular vibrational relaxation dynamics in the monomeric water systems.

IV. CONCLUSION

In this report, we investigated the vibrational relaxation dynamics of monomeric water molecule dissolved in d-chloroform solution using the 2D IR spectroscopy. The vibrational lifetime of OH bending in monomeric water shows a bi-exponential decay which is different from previous report. Furthermore, a faster reorientation of the OH bending in monomeric water is observed even the hydrogen bonds of monomeric water in the confined environment are much weaker than the hydrogen bonds in the bulk water. Most importantly, we are able to observe the direct vibrational energy transfer from OH stretching to OH bending in monomeric water. The vibrational energy relaxation mechanism in the monomeric water is complicated than previous thought and needs re-examined. Monomeric water dissolved in other confined systems, such as polar and nonpolar non-hydrogen bonding solvents, will be investigated in the future.

V. ACKNOWLEDGEMENTS

[1] F. Perakis, L. De Marco, A. Shalit, F. J. Tang, Z. R. Kann, T. D. Kehne, R. Torre, M. Bonn, and Y. Nagata, Chem. Rev. **116**, 7590 (2016).

[2] S. Meng, L. F. Greenlee, Y. R. Shen, and E. G. Wang, Nano Res. **8**, 3085 (2015).

[3] D. Laage, T. Elsaesser, and J. T. Hynes, Chem. Rev. **117**, 10694 (2017).

[4] Y. Levy and J. N. Onuchic, Annu. Rev. Biophys. Biomol. Struct. **35**, 389 (2006).

[5] P. Ball, Chem. Rev. **108**, 74 (2008).

[6] B. Bagchi, Chem. Rev. **105**, 3197 (2005).

[7] I. D. Jr. Kuntz and W. Kauzmann, Adv. Protein Chem. **28**, 239 (1974).

[8] S. K. Pal and A. H. Zewail, Chem. Rev. **104**, 2099 (2004).

[9] D. P. Zhong, S. K. Pal, and A. H. Zewail, Chem. Phys. Lett. **503**, 1 (2011).

[10] P. Jungwirth, J. Phys. Chem. Lett. **6**, 2449 (2015).

[11] M. C. Bellissent-Funel, A. Hassanali, M. Havenith, R. Henchman, P. Pohl, F. Sterpone, D. van der Spoel, Y. Xu, and A. E. Garcia, Chem. Rev. **116**, 7673 (2016).

[12] A. C. Fogarty, E. Duboué-Dijon, F. Sterpone, J. T. Hynes, and D. Laage, Chem. Soc. Rev. **42**, 5672 (2013).

[13] V. Helms, Chemphyschem **8**, 23 (2007).

[14] J. C. Smith, F. Merzel, A. N. Bondar, A. Tournier, and S. Fischer, Philos. Trans. R. Soc. Lond. B Biol. Sci. **359**, 1181 (2004).

[15] M. L. Berkowitz, D. L. Bostick, and S. Pandit, Chem. Rev. **106**, 1527 (2006).

[16] M. D. Fayer and N. E. Levinger, Annu. Rev. Phys. Chem. **3**, 89 (2010).

[17] M. D. Fayer, Acc. Chem. Res. **45**, 3 (2012).

[18] S. K. Pal, J. Peon, and A. H. Zewail, Proc. Natl. Acad. Sci. USA **99**, 1763 (2002).

[19] N. F. A. van der Vegt, K. Haldrup, S. Roke, J. R. Zheng, M. Lund, and H. J. Bakker, Chem. Rev. **116**, 7626 (2016).

[20] M. D. Fayer, Annu. Rev. Phys. Chem. **60**, 21 (2009).

[21] S. T. Roberts, K. Ramasesha, and A. Tokmakoff, Acc. Chem. Res. **42**, 1239 (2009).

[22] M. F. Kropman and H. J. Bakker, Science **291**, 2118 (2001).

[23] M. D. Fayer, D. E. Moilanen, D. Wong, D. E. Rosenfeld, E. E. Fenn, and S. Park, Acc. Chem. Res. **42**, 1210 (2009).

[24] G. Seifert, T. Patzlaff, and H. Graener, J. Chem. Phys. **120**, 8866 (2004).

[25] G. Seifert, T. Patzlaff, and H. Graener, J. Chem. Phys. **125**, 154506 (2006).

[26] G. Seifert and H. Graener, J. Chem. Phys. **127**, 224505 (2007).

[27] H. Graener and G. Seifert, J. Chem. Phys. **98**, 36 (1993).

[28] Y. S. Lin, S. G. Ramesh, J. M. Shorb, E. L. Sibert III, and J. L. Skinner, J. Phys. Chem. B **112**, 390 (2008).

[29] D. Cringus, T. L. C. Jansen, M. S. Pshenichnikov, and D. A. Wiersma, J. Chem. Phys. **127**, 084507 (2007).

[30] F. Dahms, R. Costard, E. T. J. Nibbering, and T. Elsaesser, Chem. Phys. Lett. **652**, 50 (2016).

[31] H. T. Bian, J. B. Li, X. W. Wen, and J. R. Zheng, J. Chem. Phys. **132**, 184505 (2010).

[32] H. T. Bian, X. W. Wen, J. B. Li, and J. R. Zheng, J. Chem. Phys. **133**, 034505 (2010).

[33] H. T. Bian, H. L. Chen, J. B. Li, X. W. Wen, and J. R. Zheng, J. Phys. Chem. A **115**, 11657 (2011).

[34] H. T. Bian, X. W. Wen, J. B. Li, H. L. Chen, S. Han, X. Q. Sun, J. Song, W. Zhuang, and J. R. Zheng, Proc. Natl. Acad. Sci. USA **108**, 4737 (2011).

[35] H. T. Bian, J. B. Li, Q. Zhang, H. L. Chen, W. Zhuang, Y. Q. Gao, and J. R. Zheng, J. Phys. Chem. B **116**, 14426 (2012).

[36] H. T. Bian, H. L. Chen, Q. Zhang, J. B. Li, X. W. Wen, W. Zhuang, and J. R. Zheng, J. Phys. Chem. B **117**, 7972 (2013).

[37] H. L. Chen, H. T. Bian, J. B. Li, X. W. Wen, and J. R. Zheng, Int. Rev. Phys. Chem. **31**, 469 (2012).

[38] H. L. Chen, H. T. Bian, and J. R. Zheng, Acta Phys. Chim. Sin. **33**, 40 (2017).

[39] H. T. Bian, J. B. Li, X. W. Wen, Z. G. Sun, J. Song, W. Zhuang, and J. R. Zheng, J. Phys. Chem. A **115**, 3357 (2011).

[40] H. T. Bian, J. B. Li, H. L. Chen, K. J. Yuan, X. W. Wen, Y. Q. Li, Z. G. Sun, and J. R. Zheng, J. Phys. Chem. C **116**, 7913 (2012).

[41] Y. L. A. Rezus and H. J. Bakker, J. Chem. Phys. **123**, 114502 (2005).

[42] I. R. Piletic, D. E. Moilanen, D. B. Spry, N. E. Levinger, and M. D. Fayer, J. Phys. Chem. A **110**, 4985 (2006).

[43] J. J. Gilijamse, A. J. Lock, and H. J. Bakker, Proc. Natl. Acad. Sci. USA **102**, 3202 (2005).